Available online at www.sciencedirect.com

ScienceDirect

Advances in Space Research 74 (2024) 5687–5697

ADVANCES IN SPACE RESEARCH (a COSPAR publication)

www.elsevier.com/locate/asr

Periodic orbits around 216-Kleopatra asteroid modelled by a dipole-segment

Alberto Abad [a,1], Antonio Elipe [a,*,1], Alessandra F.S. Ferreira [b,2]

[a] Universidad de Zaragoza, Zaragoza, Spain
[b] Universidade Estadual Paulista (UNESP), Brazil

Received 9 July 2024; received in revised form 20 September 2024; accepted 9 October 2024
Available online 16 October 2024

Abstract

Asteroid 216-Kleopatra presents a ham-bone shape, that is to say, it is quite elongated body with two protuberances on its end-points, which makes of it the perfect candidate to model its shape and mass distribution by a Dipole-Segment, consisting on a massive segment with two spherical masses at the end-points of the rod and that is rotating about its center of mass with uniform velocity. Once obtained an approximation of the actual values of the involved parameters from recent results of Burov and coworkers, we obtain the complete map of families of symmetric periodic orbits, and describe the orbits of the different families, its parametric evolution, stability and also we compute the heteroclinic orbits connecting unstable isosceles equilibria.

Keywords: Orbital dynamics; Families of periodic orbits; Asteroid gravitational potential; Dipole-Segment gravitational field

1. Introduction

Minor bodies in the Solar system, like asteroids, comets and planetary moons, are currently studied to better understanding the evolution of our solar system, and space missions to them opened a door to a fruitful research field in Astrodynamics where new assumptions and methods are required. Indeed, one of the main characteristics of these bodies is their irregular shape, mass distribution, and rotation.

The traditional way of representating the gravity potential by means of expansions in Legendre polynomials series is no longer valid when the body is far of having an almost spherical shape, such as happens with many asteroids, which have irregular shape and even irregular distribution of masses. To circumvent this difficulty, several models have been proposed, thus, a very complete model is to consider a homogeneous polyhedron (Werner, 1994; Werner and Scheeres, 1997). However, although complete, this model presents many free parameters, which adds an amount of complexity to its use.

For elongated asteroids, much simpler models have been proposed, thus, we find the one proposed by Prieto-Llanos and Gómez-Tierno (1994) consisting of a rotating two-fixed-centers system, model considered later on by Zeng and Liu (2017). An extension of this model has been done by Palacios et al. (2019) who add a third central body in such a way the three bodies are aligned. Another and very interesting model specially for very elongated bodies consists in assuming the body a finite straight segment (Halamek, 1988; Riaguas, 1999; Elipe and Riaguas, 2003). This model results very attractive, because it is simple and, which is very important, the potential is expressed

* Corresponding author.
E-mail address: elipe@unizar.es (A. Elipe).
[1] Instituto Universitario de Matemáticas y Aplicaciones, Spain.
[2] Departmen of UNESP, Brazil.

https://doi.org/10.1016/j.asr.2024.10.017
0273-1177/

in closed form in terms of a logarithm with intrinsic quantities, namely the distance of the orbiting point to the endpoints of the segment and its length, and hence, there is no need to approximate it by means of series expansions. To our knowledge, Duboshin (1959) was the first one in considering such a body although in his paper, the segment was used to model a spacecraft orbiting an spherical central body. In our case, we assume the massive segment to be part of the central body. The problem of the rotating segment has been extensively analyzed by Elipe and coworkers; thus, the analysis of the non-lineal stability of the equilibria (Elipe et al., 2001; Riaguas et al., 2001), the finding of periodic orbits (Riaguas et al., 1999; Riaguas, 1999) and even the proof of the non integrability of the problem (Arribas and Elipe, 2001), which gives some indications about the chaoticity of the motion at some energy levels. This fact was used to compute regions of stability-chaos for orbits around an elongated body like 433-Eros asteroid (Elipe and Lara, 2003). To have a more accurate representation of the potential of elongated bodies, not necessarily thin, Breiter and collaborators (Bartczak and Breiter, 2003; Bartczak et al., 2006) consider two perpendicular segments, which is an alternative simple model for a two-axial and a three-axial ellipsoid. Recently, Gutiérrez et al. (2024) propose a variable density segment, represented by a second degree polynomial linear density, rotating around its center of mass.

But there are other asteroids with peculiar shapes, for instance 216-Kleopatra asteroid that has a ham-bone-shaped shape (see Fig. 1) and that needs a different approach to model it. An extension to the rectilinear segment and to the two-fixed-centers or dipole, introduced by Zeng et al. (2018), consists of merging both moldels by adding the spheres of the dipole to the end points of the segment, resulting thus the *Dipole-Segment* model, hereafter the DS model. With this model, Zeng et al. (2018) obtain the Hamiltonian, find numerically the equilibria and provide some 3D graphics with the linear stability; with these results, Zhang et al. (2018) apply the DS system to model several elongated asteroids and carry out a comprehensive study of three-dimensional periodic orbits around a DS, by using the hierarchical gridding method presented in Zeng and Alfriend (2017) and make a topological classification of the 3-D periodic orbits, based on the classification given in Jiang et al. (2015).

One of the main advantages of this model, as proven in (Zeng et al., 2018; Zhang et al., 2018), is that the DS system potential is expressed in closed form, because it is made of the addition of two closed form expressions, the dipole (Prieto-Llanos and Gómez-Tierno, 1994) and the massive segment (Duboshin, 1959).

From our part, we extended the work of Zeng et al. (2018) by finding a map of symmetric periodic orbits when both Dipole's masses are equal (Elipe et al., 2021). The problem depends on three parameters, namely the mass ratio of the Dipole (μ), the Segment mass (μ_s), and the angular rotation (κ) of the DS system. In Elipe et al. (2021), two parameters were fixed, $\mu = 1/2$ and $\kappa = 1$, and the evolution of the families of periodic orbits was computed for $\mu_s \in [0, 1]$. Some later, Elipe et al. (2021) did a similar analysis but now for $\mu = 1/2, \mu_s = 0.3$, and the evolution of the families of periodic orbits is performed with respect to the rotation parameter κ. Even recently, some authors (Boaventura et al., 2023) used a model with a tripole and a segment to better approach the Holiday asteroid shape.

However the main challenge when applying the DS model is to have the actual (or a good approximation) values of physical parameters for specific asteroids. In this paper, we are interested in finding families of axis-symmetrical periodic orbits around 216-Kleopatra, thus, we need a good approximation of the involved parameters μ, μ_s, and κ. With this aim, we use the results given by Burov and coworkers (Burov et al., 2018; Burov et al., 2019; Burov et al., 2018) who by using the K-means method are able to split an irregular body into several balls, generally three (Burov et al., 2019) or four (Burov et al., 2018) spheres. Fortunately for us, 216-Kleopatra asteroid was one of the cases analyzed in Burov et al. (2019), which helped us in determining the values of the parameters in the DS model (Section 3).

In Section 2 we briefly describe the potential of the DS body, introduce the three parameters involved on it, and obtain the equations of motion of a spacecraft around

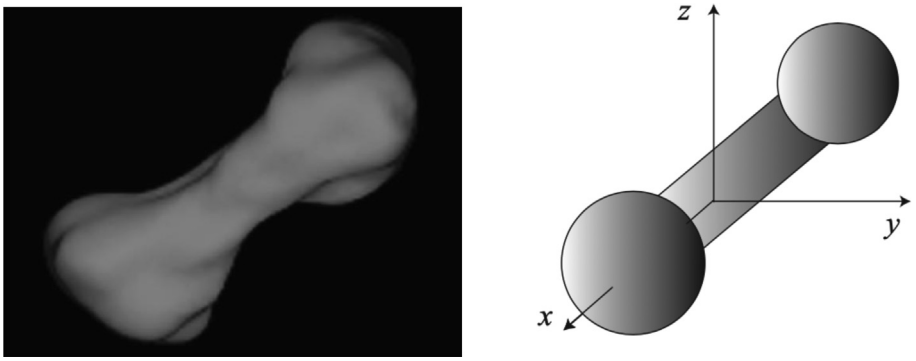

Fig. 1. Left: Image of the 216-Kleopatra asteroid, by NASA. Right: Scheme of the Dipole-Segment (DS) system.

the DS in a synodic reference frame and the expression of Jacobian constant. In Section 3, for the specific values of the parameters for Kleopatra asteroid, we determine the position of the equilibria and their stability. Next, in Section 4, we proceed to the computation of the whole set of natural families of planar symmetric periodic orbits by using the so-called *grid-search* method and also the stability regions of each family, because the knowledge of these bifurcations is of capital importance in computing families of 3-D periodic orbits (Tresaco et al., 2013).

2. Potential of the DS problem and equations of motion

Let $OXYZ$ be an inertial reference frame. Let us also consider the body made of two points (or spherical bodies) of masses m_1 and m_2 joined by a segment of mass m and length ℓ with constant linear density of mass ρ. This body is rotating uniformly on the XY-plane with constant angular velocity ω about its center of masses O. This system will be called Dipole-Segment (DS). Because the DS system is rotating, we define a synodic frame $Oxyz$ in such a way the $OZ = Oz$ and the body is permanently rotating on the axis Ox. We are interested on the motion of an infinitesimal mass P under the gravitational field of the DS system.

Let us denote

$$M = m_1 + m_2 + m, \quad \mu = \frac{m_2}{m_1 + m_2},$$
$$(1-\mu) = \frac{m_1}{m_1 + m_2}, \quad \mu_s = \frac{m}{M}, \tag{1}$$

and

$$(-\ell_1, 0, 0), \quad (\ell_2, 0, 0), \quad \text{with} \quad \ell_1 + \ell_2 = \ell$$

the coordinates of masses m_1 and m_2 in the $Oxyz$ frame. With this we have

$$\frac{m_1}{M} = (1-\mu)(1-\mu_s), \quad \frac{m_2}{M} = \mu(1-\mu_s).$$

Note that if $\mu_s = 0$, there is no segment and we have the classical Two-Center or Dipole Problem; when $\mu_s = 1$ ($\Longleftrightarrow m_1 = m_2 = 0$) we only have the segment; if $\mu = 0$ ($\Longleftrightarrow m_2 = 0$) there is only the mass m_1 at the left extreme of the segment, while if $\mu = 1$ ($\Longleftrightarrow m_1 = 0$) there is only the mass m_2 at the right end of the segment.

Because of the fact that the origin O is at the center of mass of the system, there results that

$$\begin{aligned} \tfrac{\ell_2}{\ell} &= \tfrac{1}{M}\left(m_1 + \tfrac{m}{2}\right) = (1-\mu)(1-\mu_s) + \tfrac{1}{2}\mu_s, \\ \tfrac{\ell_1}{\ell} &= \mu(1-\mu_s) + \tfrac{1}{2}\mu_s. \end{aligned} \tag{2}$$

With this, the potential function is

$$U = -\mathcal{G}M\left(\frac{(1-\mu)(1-\mu_s)}{r_1} + \frac{\mu(1-\mu_s)}{r_2} + \frac{\mu_s}{\ell}\log\left[\frac{r_1 + r_2 + \ell}{r_1 + r_2 - \ell}\right]\right),$$

where $\mathcal{G}$ is the gravitation constant, $r_1 = \|P_1P\|$ and $r_2 = \|P_2P\|$, that is,

$$r_1^2 = (x+\ell_1)^2 + y^2 + z^2, \quad r_2^2 = (x-\ell_2)^2 + y^2 + z^2.$$

Next, we make two unit scaling, namely time ($t \longrightarrow \omega t$) and length ($r \longrightarrow \ell r$), which is equivalent to choose ℓ as unit of length and $1/\omega$ as unit of time (Elipe et al., 1992). After scaling, the equations of motion in the synodic frame are

$$\begin{aligned} \ddot{x} - 2\dot{y} &= x - \tfrac{1}{\omega^2}\tfrac{\partial U}{\partial x} = \tfrac{\partial \Omega}{\partial x}, \\ \ddot{y} + 2\dot{x} &= y - \tfrac{1}{\omega^2}\tfrac{\partial U}{\partial y} = \tfrac{\partial \Omega}{\partial y}, \\ \ddot{z} &= -\tfrac{1}{\omega^2}\tfrac{\partial U}{\partial z} = \tfrac{\partial \Omega}{\partial z}, \end{aligned} \tag{3}$$

where Ω is the effective potential

$$\begin{aligned} \Omega &= \tfrac{1}{2}(x^2+y^2) - \tfrac{1}{\omega^2}U \\ &= \tfrac{1}{2}(x^2+y^2) + \kappa\left(\tfrac{(1-\mu)(1-\mu_s)}{r_1} + \tfrac{\mu(1-\mu_s)}{r_2} + \mu_s \log\left[\tfrac{r_1+r_2+1}{r_1+r_2-1}\right]\right), \end{aligned} \tag{4}$$

and the dimensionless parameter

$$\kappa = \frac{1}{\omega^2}\frac{\mathcal{G}M}{\ell^3} \in (0, \infty) \tag{5}$$

is the ratio of gravitational acceleration to centrifugal acceleration. Thus, the problem depends on three dimensionless parameters μ, μ_s and κ. Details on the obtaining of the above expressions can be found in (Elipe and Riaguas, 2003; Riaguas et al., 2001; Zeng et al., 2018; Elipe et al., 2021) When $\mu_s = 0$ (the two fixed-center problem) and $\kappa = 1$, we have the RTBP. When $\kappa < 1$ the segment rotates fast, whereas $\kappa > 1$ means slow rotation. As it was pointed out by Prieto-Llanos and Gómez-Tierno (1994), for fast rotations, cohesive strength is necessary to avoid body disruption under forces of inertia unbalanced by body self-gravitation, which implies that the case $\kappa \ll 1$ is not very realistic. On the contrary, slow rotation case seems to be the most common case, in which some compressive strength prevents the body from collapsing to adopt the shape of an oblate spheroid.By using the notation of Riaguas et al. (2001), $s = r_1 + r_2$, $d = r_1 - r_2$, $p = r_1 r_2$, the equations of motion become

$$\begin{aligned} \ddot{x} - 2\dot{y} &= \tfrac{\partial \Omega}{\partial x} = \tfrac{\kappa(1-\mu_s)}{2}\left(\tfrac{(x+\ell_1)}{r_1^3} + \tfrac{(x-\ell_2)}{r_2^3}\right) - \left(1 - \tfrac{2\kappa\mu_s}{sp}\right)x, \\ \ddot{y} + 2\dot{x} &= \tfrac{\partial \Omega}{\partial y} = \left[\tfrac{\kappa(1-\mu_s)}{2}\left(\tfrac{1}{r_1^3} + \tfrac{1}{r_2^3}\right) - \left(1 - \tfrac{2\kappa\mu_s s}{(s^2-1)p}\right)\right]y, \\ \ddot{z} &= \tfrac{\partial \Omega}{\partial z} = \kappa\left[\tfrac{(1-\mu_s)}{2}\left(\tfrac{1}{r_1^3} + \tfrac{1}{r_2^3}\right) + \tfrac{2\kappa\mu_s s}{(s^2-1)p}\right]z, \end{aligned} \tag{6}$$

where ℓ_i are expressed in terms of the parameters by Eq. (2).As it is usual with problems formulated on a synodic frame, equations of motion (3) have as a first integral the so-called Jacobian constant C given by

$$C = 2\Omega - (\dot{x}^2 + \dot{y}^2 + \dot{z}^2), \tag{7}$$

which provides useful information on the dynamics, such as forbidden regions for the motion, because $C \geqslant 2\Omega$.

3. (216) Kleopatra case

One of the most conspicuous cases where the shape of an asteroids may be modelled by the DS system is the main-belt asteroid (216) Kleopatra. Indeed, Ostro et al.

(2000) performed very accurate radar observations and inferred a three-dimensional reconstructed shape similar to a dog-bone, with dimensions of $217 \times 94 \times 81$ km and an equivalent radius of 54.25 ± 7 km (radius of a sphere with the same volume as the shape model), and that is spinning about its major principal axis of inertia with a period of 5.385 h, which has been widely used ever since. Later on, Descamps et al. (2011) improved the observations and confirmed that asteroid's shape was a very long body with two protuberances at each end, that is, it looks like a dumbbell shape. In addition, they discovered that Kleopatra has two 5–10 km diameter moonlets whose orbits, allowed them to estimate Kleopatra's mass (see Table 1). However, to use the DS model, we need not only the total mass of the body, but the individual masses of the segment and of the two protuberances. To this end, we use the results given by Burov et al. (2018, 2019, 2018) who use the so-called *K*-means method based on Steinhaus's theory (Steinhaus, 1956). Briefly, they consider that asteroids are approximated by homogeneous polyhedra given by sets of vertices of triangular face (Werner, 1994); then, they make a partition of three subsets (centers of balls) that are the vertices of a triangle with sides d_i such that $d_1 : d_2 : d_3 = 1 : 1.258 : 2.253$, and the angles α_i (opposite to side d_i) are $\alpha_1 = 0.05986419570, \alpha_2 = 0.07533678312$, and $\alpha_3 = 3.006391676$. In so doing, they determine the three masses of the components of the DS that appear in Table 1 and which allow us to fix the values of the three parameters κ, μ and μ_s. Note that because $\kappa = 0.991 < 1$, the DS has a moderate fast rotation. Fast spinning plays an important role in the structure of asteroids. Hirabayashi and Scheeres (2014) made an analysis of the surface shedding, that is, of the dynamical process of small particles on the surface and found that fast spinning originate the motion of particles on the surface towards the extremities of the minor principal axis of inertia, and eventually, if the spin is increasing, the particle may abandon the main body. This fact may explain the origin of the two Kleopatra's moons (Descamps et al., 2011; Hirabayashi and Scheeres, 2014). Once DS parameters fixed, and for planar motions $(x, y, 0)$, let us plot the surface $C = 2\Omega(x, y)$ and its level contours, that is to say, the zero velocity curves $C = 2\Omega(x, y)$ for constant values of the Jacobian constant C. Both graphics appear in Fig. 2. From the plots, it seems that there are four equilibria, two on the x-axis (apparently unstable) and other two on the vertical line, $x = 0.0123334$. It is worth noticing that unstable equilibria on the x-axis are not connected, that is, both are on different zero velocity curves and then the value of the Jacobian constant at one of these points is different to its value at the other one. We shall prove it once we have the coordinates of equilibria.Equilibria are obtained by zeroing the equations of motion (6). It can be easily checked that the only solution for $\ddot{z} = 0$ is $z = 0$, because in the third equation of (6) the coefficient of z is always strictly positive. With this, the possible equilibria are on the plane Oxy. To find them, we solve the system made by equating to zero the first two equations of Eq. (6) with $z = 0$. It is easy to realize (Elipe et al., 2021) that there are two types of equilibria, two on the Ox-axis that we denote *collinear points* (L_1, L_2) and other two points forming isosceles triangles with the primaries, that we name *triangular points* (L_4, L_5). Because of the symmetry, the behavior of both triangular points is the same, thus, along the paper we shall use the name triangular points (T) to designate these equilibria.The solution of the system for the parameters corresponding to Kleopatra appears in Table 2. Note that the Jacobian constant at points L_1 and L_2 takes different values $(C(L_1) \neq C(L_2))$, hence equilibria L_1 and L_2 are on different zero velocity curves, as just mentioned in the previous paragraph. The linear stability is obtained by means of the linearized equations of (6). The variational matrix is

$$A = \begin{bmatrix} 0 & 0 & 1 & 0 \\ 0 & 0 & 0 & 1 \\ \Omega_{xx} & \Omega_{xy} & 0 & 2 \\ \Omega_{xy} & \Omega_{yy} & -2 & 0 \end{bmatrix},$$

where the partial second derivatives must be evaluated at the equilibria. Its eigenvalues for the four equilibria are also given in Table 2. Note that all equilibria have at least one eigenvalue with real part strictly positive, then, we conclude that the four equilibria are unstable.

Table 1
Physical data and parameters of (216) Kleopatra.

m_1 (kg)	m_2 (kg)	m_s (kg)	ℓ (m)	T (h)
1.1014×10^{18}	1.0350×10^{18}	4.1547×10^{17}	117800	5.385
κ	μ	μ_s	ℓ_1	ℓ_2
0.991	0.484	0.163	0.486608	0.513392

4. Symmetric periodic orbits

Next, we look for families of periodic orbits on the plane Oxy that are symmetric with respect to the Ox-axis, hence, these orbits orthogonally cross the Ox-axis twice per period. In consequence, if we take as initial time $(t_0 = 0)$ the instant at the perpendicular crossing of Ox-axis, the initial coordinates of the particle are $(x_0, 0, 0, \dot{y}_0)$, and after half period $(T/2)$ the coordinates will be $(x_{T/2}, 0, 0, \dot{y}_{T/2})$. Thus, to find a symmetric periodic orbit from any set of initial conditions $(x_0, 0, 0, \dot{y}_0)$ we have to find the instant $(T/2)$ of the next perpendicular crossing of the orbit

$$y(x_0, 0, 0, \dot{y}_0; T/2) = 0, \qquad \dot{x}(x_0, 0, 0, \dot{y}_0; T/2) = 0.$$

If we accomplish that, the orbit with these initial conditions is symmetric and T-periodic.

There are many different procedures to find such initial conditions. We shall follow the *grid search method*, term coined by (Markellos et al., 1974) who described in a systematic way how to compute families of symmetric periodic orbits. This method was already outlined by Strömgren (1933) in his monumental work in the so called *Copenhagen*

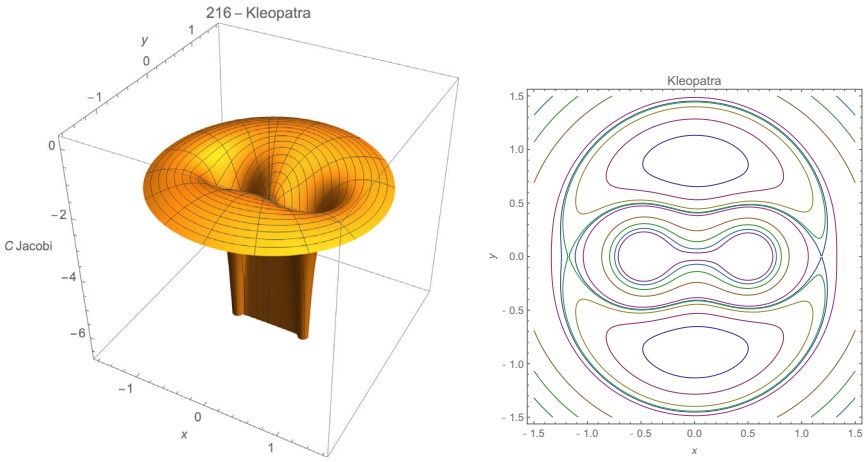

Fig. 2. Left) The zero velocity surface $-C = -2\Omega(x, y)$. Right) the zero velocity curves for the chosen parameters of 216-Kleopatra.

Table 2
Coordinates and stability of the equilibria for (216) Kleopatra and values of the Jacobian constant at these points.

	Coordinates	Eigenvalues	Stability	$C(L_j)$
L_1	$(-1.176968, 0)$	$\pm 1.309601\,\mathrm{i}, \pm 1.113645$	unstable	3.389503
L_2	$(1.185509, 0)$	$\pm 1.326267\,\mathrm{i}, \pm 1.150075$	unstable	3.406430
L_4	$(0.012333, 0.882277)$	$\pm 0.600538 \pm 0.927710\,\mathrm{i}$	unstable	2.763408
L_5	$(0.012333, -0.882277)$	$\pm 0.600538 \pm 0.927710\,\mathrm{i}$	unstable	2.763408

problem, and was improved some years later by Hénon (1965). Details of the method may be found, for instance, in (Markellos et al., 1974; Elipe et al., 2007; Palacios et al., 2019; Abad et al., 2023) and references therein.

Briefly, it consists on the following. Because of the existence of Jacobi's constant (7), it is possible to put $\dot{y}_0^2 = 2U(x_0) - C$, hence we will locate the initial conditions on the plane (x_0, C) instead of $(x_0, \dot{y}_0)$. We build a regular mesh $(x_j, C_j), j = 0, \ldots, N$, on the plane (x, C); next we take from the mesh two consecutive points (x_i, C_k) and (x_{i+1}, C_k) and for these two sets of initial conditions we integrate equations of motion (6) until the orbit crosses again the Ox-axis ($\Longleftrightarrow y_i(T_i/2) = 0$ and $y_{i+1}(T_{i+1}/2) = 0$). Then, we check whether the product $\dot{x}_i(T_i/2) \cdot \dot{x}_{i+1}(T_{i+1}/2) < 0$, that is, whether they have opposite signs. If not, we move to the next point on the grid and repeat the process. If affirmative case, by continuity, there is an intermediate point (x_i^*, C_k) with $x_i < x_i^* < x_{i+1}$ such that $\dot{x}_i(T_i/2) = 0$, i.e., the orbit crosses orthogonally the abscissas axis, and consequently, the orbit is symmetric and periodic. We keep this point and move to next point on the mesh until the whole grid is scanned. The finding of points x_i^* is achieved by means of Brent's method (Brent, 1971) because it is fast and always converges. In propagating the orbit we use a Taylor series method (Abad et al., 2011; Abad et al., 2012; Lara et al., 1999) which allows us extended precision, quite convenient in bifurcation cases.

By applying the grid search method to our problem, we find five different families (continuous curves in map) of symmetric periodic orbits for Kleopatra asteroid, which we name m, l, b, k, and a families, represented in Fig. 3. We name the families by using the classical naming given by Strömgren (1933) in the RTBP and extended by Hénon (1965, 1997).

Plots are on the plane of initial conditions (x, C); grey areas correspond to forbidden regions of motion according to Jacobian constant. Note that in the graphics there are two asymptotic (also called spiral) points, one on each region Z_l and Z_r; these asymptotic points correspond to heteroclinic orbits connecting the two unstable isosceles points. These heteroclinics are: one stable orbit $\mathcal{S}$ and the other unstable $\mathcal{U}$ with respect to the triangular point L_4, that is to say, orbit $\mathcal{S}$ starts in L_5 and ends in L_4 (the intersection of stable $W^S(L_4)$ and unstable $W^U(L_5)$ manifolds), whereas orbit $\mathcal{U}$ goes from L_4 to in L_5 (the intersection $W^U(L_4) \cap W^S(L_5)$).

To describe the orbits along the different families, we shall use with slight modifications the notation introduced by Abad et al. (2023) in the Restricted Three Body Problem (RTBP).

The isoenergetic exploration reduces the system to a symplectic map of the plane $(x, \dot{x})$ and the Jacobian matrix of the map is often represented as

$$J = \begin{pmatrix} a & b \\ c & d \end{pmatrix} = \begin{pmatrix} \partial x/\partial x_0 & \partial x/\partial \dot{x}_0 \\ \partial \dot{x}/\partial x_0 & \partial \dot{x}/\partial \dot{x}_0 \end{pmatrix}.$$

The eigenvalues of this matrix play a major role in discussing the stability of the orbits (Hénon, 1965; Broucke and Elipe, 2005). Indeed, the trace of this matrix $k = a + d$ is called *stability index*. It was shown by Hénon

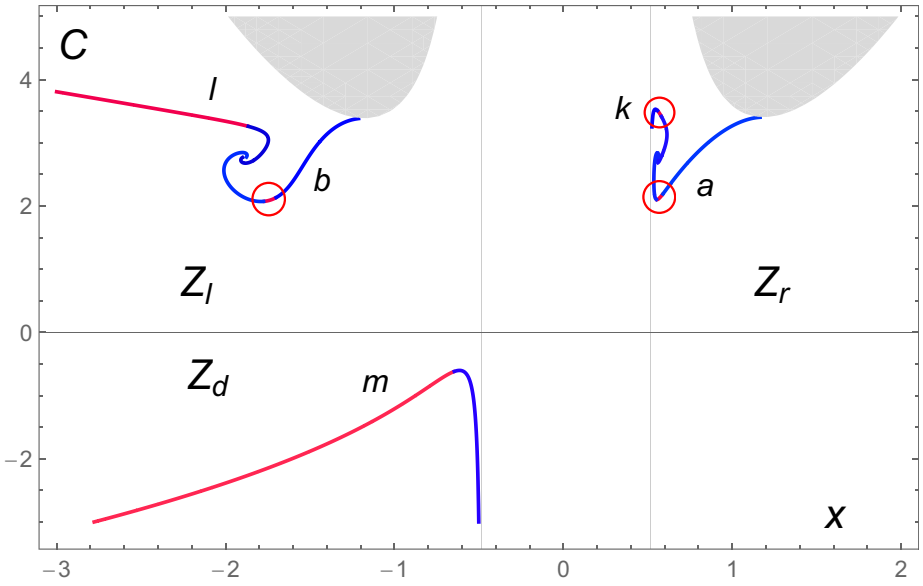

Fig. 3. Families of symmetric periodic orbits of Kleopatra asteroid. Each point of the plots on the plane (x, C) corresponds to the initial conditions of a periodic orbit. The grey shadow areas correspond to forbiden regions of motion. Pieces in red correspond to stable orbits, whereas curves in blue are made of unstable orbits. We encircle three narrow pieces in characteristic curves b, k, and a, to highlight the stable orbits in those curves.

(1965) that the stability boundaries are $k = +2$, (two eigenvalues of $+1$) and $k = -2$, (with two eigenvalues of -1). The condition of symmetry gives $a = d$, hence the stability condition is simply $|a| < 1$, and this is the criterion used along the paper.

We distinguish the stable (unstable) character of orbits within their families in Fig. 3 by switching the color, thus, red color stands for stable orbits, whereas blue color means unstable orbits. The intervals of stability of the five families in the (x, C)-plane are given in Table 3. Note that both families l and m have a wide region of stability, and them change to another wide region of instability. However, the other three families (b, a, and k) are unstable almost everywhere, except a narrow region where the families are stable.

We name direct orbits those that are described in the same sense as the rotation of the synodic coordinate system and retrograde orbits those that are described in the opposite sense; in other words, the orbit will be direct if $x_0 > x_{T/2}$ and retrograde if $x_0 < x_{T/2}$.

Let us briefly describe the orbits of these families.

∗ **Family** m**)**

Table 3
Stability of the different families in the (x, C)-plane. Families are unstable outside these values.

Family	Values (x, C) of the	
	First stable orbit	Last stable orbit
m	beginning of family	$(-0.614568, -0.602054)$
l	beginning of family	$(-1.883784, 3.273523)$
b	$(-1.783933, 2.071702)$	$(-1.724056, 2.104207)$
a	$(0.554386, 2.101602)$	$(0.571144, 2.130848)$
k	$(0.545702, 3.531726)$	$(0.569123, 3.469138)$

The family is of type $\mathcal{R}(\mathrm{DS})[\{L_1, L_2, T\} \rightarrow]$, that is, orbits are retrograde and all of them contain the Dipole-Segment DS; at the beginning of the family (left part of curve m in Fig. 3) the orbits also surround the collinear points L_1, L_2, and the isosceles points T (orbit O_1 of Fig. 4). Next, moving to the left on the x-axis of Fig. 3,

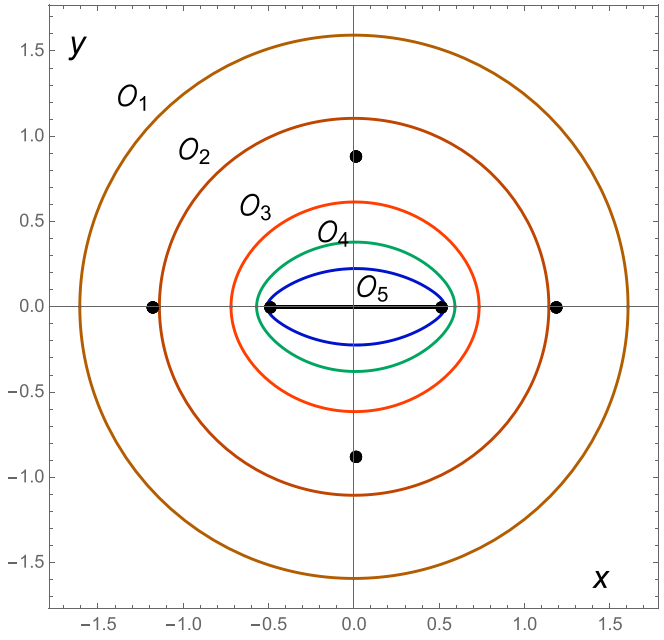

Fig. 4. Periodic orbits of family m. It is of the type $\mathcal{R}(\mathrm{DS})[\{L_1, L_2, T\} \rightarrow]$, that is, retrograde orbits and all of them have the DS in its interior. At the beginning (O_1) the orbit contain also the four equilibria (L_1, L_2, T); as we move along the family (O_2), the orbit does not contain points L_1, L_2, and eventually, orbits O_3, O_4 and O_5 only contain the DS. Note that orbits O_1, O_2 and O_3 are stable (red part of family m in Fig. 3) and that orbits O_4 and O_5 are unstable.

the orbit O_2 surrounds the triangular points and the DS, and eventually orbits only encircle the DS. Precisely, orbit O_3 is the last stable orbit of the family for increasing values of x; its initial conditions are $(x, C) = (-0.614568, -0.602054)$. For $x > -0.614568$, all orbits of family m are unstable and they are closer and closer to the DS (orbits O_4 and O_5).

∗ **Family** *l***)**

It is of the type $\mathcal{R}(L_1, \mathrm{DS}, L_2)[\rightarrow \{T, (\mathcal{S}_n\mathcal{U}_p)\}]$. Orbits are retrograde and all of them contain the Dipole-Segment and the collinear equilibria. The family begins with stable orbits (O_1, O_2 and O_3) (left part in red of family l in Fig. 3) that also surround the triangular points (see left plot of Fig. 5). Precisely, O_3 is the last stable orbit of the family as x increases. The bifurcation (transition from stability-instability) occurs at point $(x, C) = (-1.883784, 3.273523)$. The rest of the family is made of unstable orbits (O_4), similar to the previous ones, but eventually, orbits of the family evolve to orbits that make a loop around the triangular points and the family ends in two heteroclinic orbits $\mathcal{S}_n$ and $\mathcal{U}_p$ (right plot of Fig. 5).

∗ **Family** *b***)**

It is made of retrograde orbits $\mathcal{R}(L_1)[\rightarrow \{T, (\mathcal{S}_n\mathcal{U}_n)\}]$, unstable most of them. Initially, periodic orbits only contain on their interior the equilibrium L_1 (see Fig. 6, left), that is, Lyapunov orbits already described by Zhang et al. (2018) in the DS problem; they have a *half-moon* shape which is more evident as they approach the Dipole-Segment (orbits O_1, O_2), and suddenly these Lyapunov orbits become stable (e.g. orbit O_s), but only for a short arc of the family; them periodic orbits change again stability to instability. At a certain value of (x, C) of family b, orbits also surround the triangular points (see orbits O_3 and O_4), and the family ends up with two heteroclinics $\mathcal{S}_n$ and $\mathcal{U}_n$, that are plotted on the right part of Fig. 6.

∗ **Family** *a***)**

Again, all orbits of this family are retrograde and also unstable almost everywhere. Family evolution is almost the same as in family b, but switching L_1 by L_2 and orbits are almost y-symmetrical each other (see Figs. 6 and 7). This family is of type $\mathcal{R}(L_2)[\rightarrow \{T, (\mathcal{S}_p\mathcal{U}_p)\}]$, that is to say, unstable retrograde orbits containing the collinear point L_2 (Lyapunov orbits), starting with orbits very close to it (see in Fig. 7, left part, orbits O_1 and O_2). At some values of the characteristic curve, orbits become stable (orbit O_s), but soon after orbits are unstable (orbits O_3 and O_4) and the size of family's orbits increases until they contain both triangular equilibria. The limit of the family are the heteroclinics $\mathcal{S}_p$ and $\mathcal{U}_p$ (Fig. 7, right plot).

∗ **Family** *k***)**

All periodic orbits of this family are direct and unstable almost everywhere, of the type $\mathcal{D}(\mathrm{DS})[\rightarrow \{T, (\mathcal{S}_p\mathcal{U}_n)\}]$. That is, all orbits surround the DS; at the beginning the orbits are unstable and very close to the DS (orbit O_1 of Fig. 8). As we move along the family, orbits still are close to the dipole and there is a narrow piece of the characteristic curve of the family with stable orbits (like orbit O_s), orbits move away from the central part of the segment becoming unstable again (orbit O_2), until the orbits encircle the triangular points (orbit O_3), and eventually tend asymptotically to the heteroclinics $\mathcal{S}_p$ and $\mathcal{U}_n$. Note that orbits of this family k are only x-symmetric, even though they look like to be also y-symmetric.

∗ **Heteroclinic orbits**

According to Theorem 2 of (Henrard, 1973), for each pair of heteroclinic orbits, one of type $\mathcal{U}$ and the other of type $\mathcal{S}$, there is a family of periodic orbits tending asymptotically to this pair of orbits. We see in the initial conditions map (Fig. 3), that the limit of the families l and b in the zone Z_l, and k and a in the zone Z_r tend (each pair)

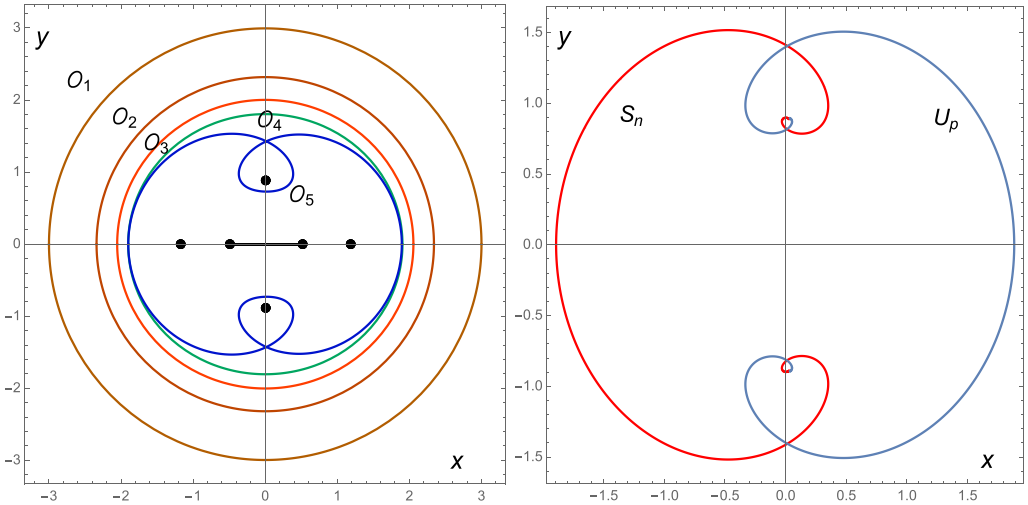

Fig. 5. Periodic orbits of family l. Are of the type $\mathcal{R}(L_1, \mathrm{DS}, L_2)[\rightarrow \{T, (\mathcal{S}_n\mathcal{U}_p)\}]$; retrograde orbits, all of them containing both collinear points and the DS. At some instant, orbits of the family (like O_5) make a loop around triangular points. From O_1 to O_3 orbits are stable. Beyond O_3 orbits are unstable. On the right part, we plot the two heteroclinic orbits $\mathcal{S}_n$ and $\mathcal{U}_p$.

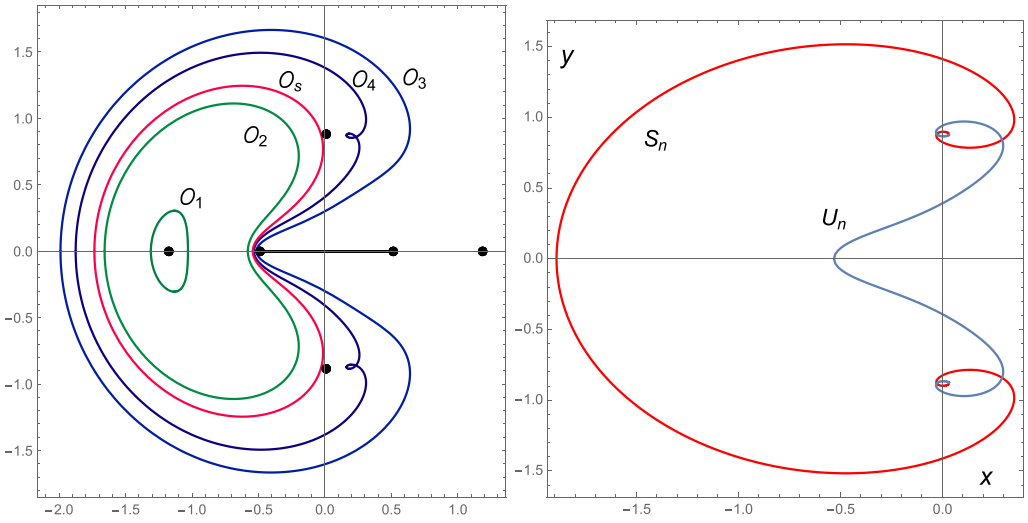

Fig. 6. Periodic orbits of family b. These orbits are unstable of $\mathcal{R}(L_1)[\rightarrow \{T, (\mathcal{S}_n\mathcal{U}_n)\}]$ type. The family starts with orbits very close to the collinear point L_1 (Lyapunov orbits); then the size increases until the orbit contain the triangular points on its interior. Lastly, orbits asymptotically tend to the heteroclinics $\mathcal{S}_n$ and $\mathcal{U}_n$.

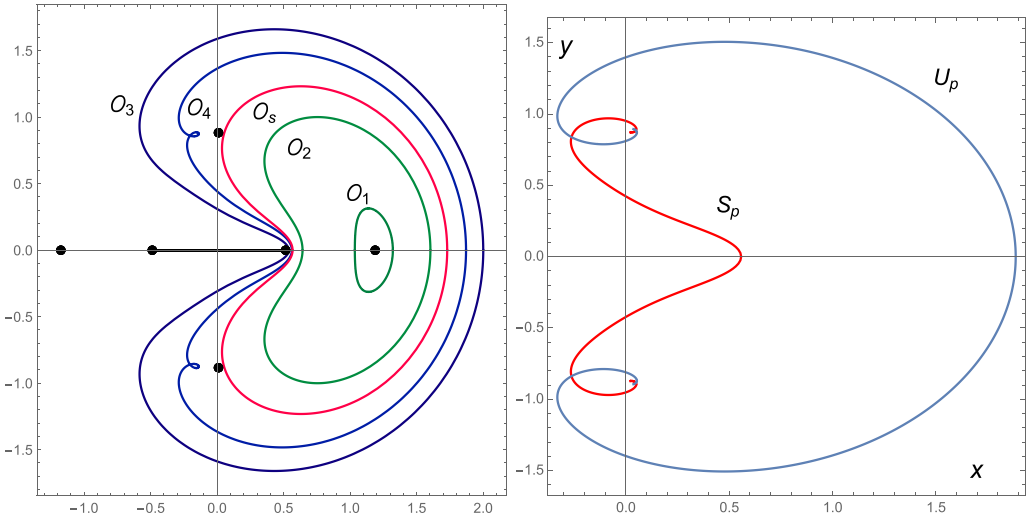

Fig. 7. Periodic orbits of family a, which is made of orbits of type $\mathcal{R}(L_2)[\rightarrow \{T, (\mathcal{S}_p\mathcal{U}_p)\}]$. Note that these orbits and those of family b are almost y-symmetrical each other.

to a single point, and these families form a spiral around this point. This point is called *asymptotic point*, and its presence is one of the characteristics of the existence of heteroclinic orbits (it is noteworthy that the non-existence of this point on the map does not imply that there are no heteroclinic orbits). The coordinates in the (x, C)-map are (x_a, C_a), where x_a is the value of the coordinate x where the heteroclinic orbit cuts the Ox-axis (in the frame $Ox\dot{x}$), and C_a is the value of the Jacobian constant evaluated at the isosceles equilibrium point, that in our case is $C_a = 2.763408$ as Table 2 shows. For details on how computing heteroclinic orbits, the reader is addressed to reference (Abad et al., 2023).

In Fig. 9 we present the heteroclinic orbits for the case of Kleopatra. Where $\mathcal{U}_n$ and $\mathcal{U}_p$, are the orbits that belongs to the set of unstable manifolds, i.e., orbits leaving the L_4 equilibrium point, and their corresponding $\mathcal{S}_n$ and $\mathcal{S}_p$, that belongs to the set of stable manifolds that reach the equilibrium point L_4. Their initial conditions are.

	$\mathcal{U}_n$	$\mathcal{U}_p$	$\mathcal{S}_n$	$\mathcal{S}_p$
x	−0.531141	1.886083	−1.891384	0.558328
C	2.763408	2.763408	2.763408	2.763408

Note that there are four heteroclinic orbits, and the combinations stable-unstable gives the possible pairs of the above described families:

$$\text{Fam } l \rightarrow \mathcal{S}_n - \mathcal{U}_p;\ \text{Fam } b \rightarrow \mathcal{S}_n - \mathcal{U}_n;\ \text{Fam } a \rightarrow \mathcal{S}_p - \mathcal{U}_p;\ \text{Fam } k \rightarrow \mathcal{S}_p - \mathcal{U}_n$$

as it can be seen on Figs. 5–8, respectively.

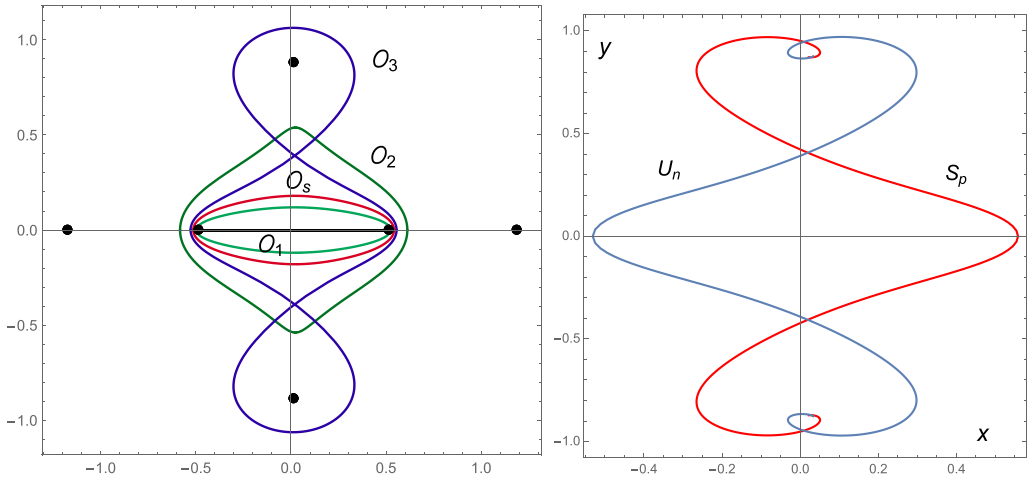

Fig. 8. Periodic orbits of family k. They are of the $\mathcal{D}(\mathrm{DS})[\rightarrow \{T, (\mathcal{S}_p\mathcal{U}_n)\}]$. The family stars with orbits very close to the DS (orbits O_1 and O_s, this one stable); next, the distance increases in the perpendicular direction to the DS (orbit O_2, unstable); eventually, orbits encircle the triangular points and tend asymptotically to the heteroclinics $\mathcal{S}_p$, and $\mathcal{U}_n$.

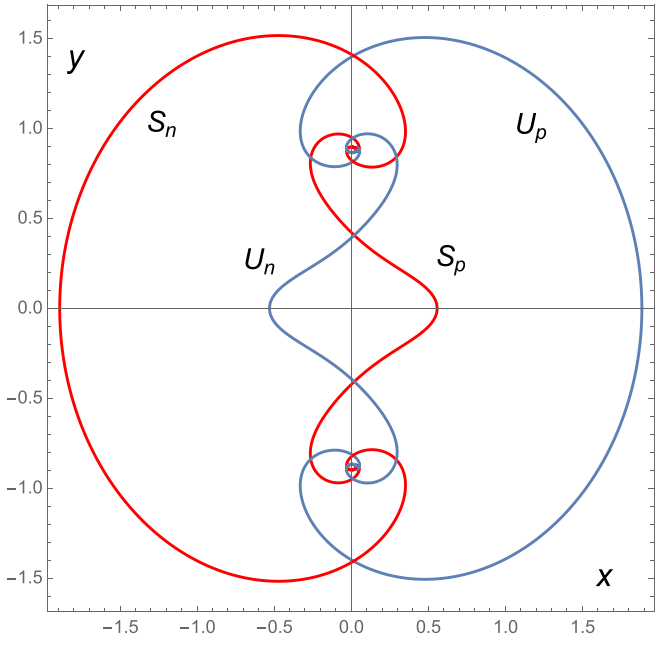

Fig. 9. The four heteroclinic orbits: the unstable $\mathcal{U}_n$ and $\mathcal{U}_p$ (in blue), ant the stable ones $\mathcal{S}_n$, and $\mathcal{S}_p$ (in red) of the Kleopatra asteroid ($k = 0.991$, $\mu = 0.484$, $\mu_s = 0.163$). (For interpretation of the references to colour in this figure legend, the reader is referred to the web version of this article.)

5. Conclusions

The Dipole-Segment system is a good model to represent the gravitational field of celestial irregular bodies like 216-Kleopatra asteroids, a quite elongated body with two protuberances on its end-points. The main advantage of this model, as proved by Zeng et al. (2018), is that the potential is expressed in closed form, with no need of further expansions.

The method given by Burov and coworkers (Burov et al., 2018) provides a nice estimation of the several parameters involved in the model, which allows us the finding of families of planar symmetric periodic orbits.

We find that there are five of those families. We describe the evolution of the orbits along each family and determine their stability and bifurcations at which there are changes of stability. Besides, we find that four families tend towards asymptotic points that correspond to heteroclinic orbits, which are also described.

Such information on the periodic orbits may be used in designing missions to this conspicuous asteroid.

Declaration of Competing Interest

The authors declare that they have no known competing financial interests or personal relationships that could have appeared to influence the work reported in this paper.

Acknowledgments

This work has been supported by Grant PID2020-117066-GB-I00 funded by MCIN/AEI/ 10.13039/501100011033, by FAPESP #2023/11781–5, and by the Aragon Government and European Social Fund (group E24-23R).

Authors are grateful to the Editor, Professor Zeng, and to the two anonymous reviewers for their comments that helped to improve the manuscript.

References

Abad, A., Arribas, M., Palacios, M., Elipe, A., 2023. Evolution of the characteristic curves in the restricted three body problem in terms of the mass parameter. Celest. Mech. Dyn. Astron. 135, 7. https://doi.org/10.1007/s10569-022-10118-z.

Abad, A., Barrio, R., Blesa, F., Rodríguez, M., 2011. TIDES tutorial: Integrating ODEs by using the Taylor series method. Mon. Real Acad. Ciencias Zaragoza, p. 36.

Abad, A., Barrio, R., Blesa, F., Rodríguez, M., 2012. Algorithm 924: TIDES, a Taylor Series Integrator for Differential EquationS. ACM Trans. Math. Software 39, 5. https://doi.org/10.1145/2382585.2382590.

Arribas, M., Elipe, A., 2001. Non-integrability of the motion of a particle around a massive straight segment. Phys. Lett. A 281, 142–148. https://doi.org/10.1016/S0375-9601(01)00124-4.

Bartczak, P., Breiter, S., 2003. Double material segment as the model of irregular bodies. Celest. Mech. Dyn. Astron. 86, 131–141. https://doi.org/10.1023/A:1024115015470.

Bartczak, P., Breiter, S., Jusiel, P., 2006. Ellipsoids, material points and material segments. Celest. Mech. Dyn. Astron. 96, 31–48. https://doi.org/10.1007/s10569-006-9017-x.

Boaventura, G.A.S., Ferreira, A.F.S., Winter, S.M.G., Winter, O.C., 2023. Analysis of symmetric periodic orbits in a tripolar system with a segment. Eur. Phys. J. Spec. Top. 232, 2297–3005. https://doi.org/10.1140/epjs/s11734-023-01036-8.

Brent, R.P., 1971. An algorithm with guaranteed convergence for finding a zero of a function. Computer J. 14, 422–425. https://doi.org/10.1093/comjnl/14.4.422.

Broucke, R.A., Elipe, A., 2005. The dynamics of orbits in a potential field of a solid circular ring. Reg. Chaotic Dynam. 10, 129–143. https://doi.org/10.1070/RD2005v010n02ABEH000307.

Burov, A.A., Guerman, A.D., Raspopova, E.A., Nikonov, V.I., 2018. On the use of the k-means algorithm for determination of mass distributions in dumbbell-like celestial bodies. Russ. J. Nonlinear Dynam. 14, 45–52, https://doi.org/10.20537/nd1801004.

Burov, A.A., Guerman, A.D., Nikonov, V.I., 2019. Using the *K*-means method for aggregating the masses of elongated Celestial Bodies. Cosmic Res. 57 (2019), 283–289. https://doi.org/10.1134/S0010952519040026.

Burov, A.A., Guerman, A.D., Nikonova, E.A., Nikonov, V.I., 2018. Approximation for attraction field of irregular celestial bodies using four massive points. Acta Astronaut. 153 (2018), 274–288. https://doi.org/10.1016/j.actaastro.2017.11.013.

Descamps, P., Marchis, F., Berthier, J., et al., 2011. Triplicity and physical characteristics of Asteroid 216-Kleopatra. Icarus 211, 1022–1033. https://doi.org/10.1016/j.icarus.2010.11.016.

Duboshin, G.N., 1959. On one particular case of the problem of the translational-rotational motion of two bodies, Sov. Astron. 3, 154–165. BibCode: 1959SvA....3.154D.

Elipe, A., Abad, A., Arribas, M., 1992. Scaling Hamiltonians in attitude dynamics. Rev. Acad. Ciencias Zaragoza 47, 147–154.

Elipe, A., Abad, A., Arribas, M., et al., 2021. Symmetric Periodic Orbits in the Dipole-segment Problem for Two Equal Masses. Astron. J. 161, 274. https://doi.org/10.3847/1538-3881/abf353.

Elipe, A., Abad, A., Ferreira, A.F.S., 2021. Dynamics of the Dipole-Segment with Equal Masses and Arbitrary Rotation, in Recent Trends in Chaotic, Nonlinear and Complex Dynamics, pp. 79–98 (2021) Chapter 4, World Sc. Ser. in Nonlinear Science Series B. pp. 79–98. doi: 10.1142/9789811221903_0004.

Elipe, A., Arribas, M., Kalvouridis, T.J., 2007. Periodic solutions in the planar $(n+1)$ ring problem with oblateness. J. Guid. Control Dynam. 30, 1640–1648. https://doi.org/10.2514/1.29524.

Elipe, A., Lanchares, V., López-Moratalla, T., Riaguas, A., 2001. Nonlinear stability in resonant cases: A geometrical approach. J. Nonlinear Sci. 11, 211–222. https://doi.org/10.1007/s00332-001-0001-z.

Elipe, A., Lara, M., 2003. A Simple Model for the Chaotic Motion Around (433). J. Astonaut. Sci. 51, 391–404. https://doi.org/10.1007/BF03546290.

Elipe, A., Riaguas, A., 2003. Nonlinear stability under a logarithmic gravity field. Int. Math. J. 3, 435–453.

Gutiérrez, J.D., Tresaco, E., Riaguas, A., 2024. Analysis in the gravitations potential of elongated asteroids. Astrophys. Space Sci. 369, 67. https://doi.org/10.1007/s10509-024-04329-z.

Halamek, P., 1988. Motion in the Potential of a Thin Bar Ph.D. dissertation. University of Texas at Austin.

Hénon, M., 1965. Exploration numérique du problème restreint. I Masses égales, Orbites periodiques, Annales d'Astrophysique 28, 499–511. BibCode: 1965AnAp...28.499H.

Hénon, M., 1997. Generating Families in the Restricted Three-Body Problem. Springer, ISBN: 3-540-63802-4.

Henrard, J., 1973. Proof of a conjecture of E. Strömgren. Celest. Mech. 7. https://doi.org/10.1007/BF01227510, 499-457.

Hirabayashi, M., Scheeres, D.J., 2014. Analysis of asteroid 216-Kleopatra using dynamical and structural constraints. Ap. J. 780, 160. https://doi.org/10.1023/A:1008233828923.

Jiang, Y., Yu, Y., Baoyin, H., 2015. Topological classifications and bifurcations of periodic orbits in the potential field of highly irregular-shaped celestial bodies. Nonlinear Dyn. 81, 119–140. https://doi.org/10.1007/s11071-015-1977-5.

Lara, M., Elipe, A., Palacios, M., 1999. Automatic programming of recurrent power series. Math. Comp. Sim. 49, 351–362. https://doi.org/10.1016/S0378-4754(99)00087-7.

Markellos, V.V., Black, W., Moran, P.E., 1974. A grid search for families of periodic orbits in the restricted problem of three todies, Celest. Mech. 9, 507–512 (1974). doi:10.1007/BF01329331.

NASA. https://apod.nasa.gov/apod/ap000510.html.

Ostro, S.J., Hudson, R.S., Nolan, M.C., et al., 2000. Radar observations of Asteroid 216-Kleopatra. Science 288, 836–839. https://doi.org/10.1126/science.288.5467.836.

Palacios, M., Arribas, M., Abad, A., Elipe, A., 2019. Symmetric periodic orbits in the Moulton-Copenhagen problem. Celest. Mech. Dyn. Astron. 131, 16. https://doi.org/10.1007/s10569-019-9893-5.

Prieto-Llanos, T., Gómez-Tierno, M.A., 1994. Stationkeeping at Libration Points of Natural Elongated Bodies. J. Guid. Control Dynam. 17, 787–794. https://doi.org/10.2514/3.21268.

Riaguas, A., 1999. Dinámica orbital alrededor de cuerpos celestes con forma irregular Ph.D. dissertation (in Spanish). Universidad de Zaragoza, Spain.

Riaguas, A., Elipe, A., Lara, M., 1999. Periodic Orbits Around a Massive Straight Segment. Celest. Mech. Dyn. Astron. 73, 69–178. https://doi.org/10.1023/A:1008399030624.

Riaguas, A., Elipe, A., López-Moratalla, T., 2001. Nonlinear stability of the equilibria in the gravity field of a finite straight segment. Celest. Mech. Dyn. Astron. 81, 235–248. https://doi.org/10.1023/A:1013217913585.

Steinhaus, H., 1956. Sur la division des corps matériels en parties. Bull. Acad. Pol. Sci. 4, 801–804, http://www.laurent-duval.eu/Documents/Steinhaus_H_1956_j-bull-acad-polon-sci_division_cmp-k-means.pdf.

Strömgren, E., 1933. Connaissance actuelle des orbites dans le problème des trois corps, Bull. Astron. 9, 87–130. BibCode: 1933BuAst...9...87S.

Tresaco, E., Riaguas, A., Elipe, A., 2013. Numerical analysis of periodic solutions and bifurcations in the planetary annulus problem. Appl. Math. Comput. 225, 645–655. https://doi.org/10.1016/j.amc.2013.10.029.

Werner, R.A., 1994. The Gravitational Potential of a Homogeneous Polyhedron or Don't Cut Corners. Celest. Mech. Dyn. Astron. 59, 253–278. https://doi.org/10.1007/BF00692875.

Werner, R.A., Scheeres, D.J., 1997. Exterior Gravitation of a Polyhedron Derived and Compared with Harmonic and Mascon Gravitation Representations of Asteroid 4769 Castalia. Celest. Mech. Dyn. Astron. 65, 313–344. https://doi.org/10.1007/BF00053511.

Zeng, X., Alfriend, K.T., 2017. Periodic orbits in the Chermnykh problem. Astrodynamics 1, 41–55. https://doi.org/10.1007/s42064-017-0004-7.

Zeng, X., Liu, X., 2017. Searching for time optimal periodic orbits near irregularly shaped asteroids by using an indirect method, IEEE Trans. Aerosp. Electron. Syst. 53, 1221–1229. https://doi.org/10.1109/TAES.2017.2668071.

Zeng, X., Zhang, Y., Yu, Y., Liu, X., 2018. The dipole segment model for axisymmetrical elongated asteroids. AJ 155, 85. https://doi.org/10.3847/1538-3881/aaa483.

Zhang, Y., Zeng, X., Liu, X., 2018. Study on periodic orbits around the dipole segment model for dumbbell-shaped asteroids. Sci. China Technol. Sci. 61, 819–829. https://doi.org/10.1007/s11431-017-9099-y.